MITOSIS DETECTION FOR STEM CELL TRACKING IN PHASE-CONTRAST MICROSCOPY IMAGES

Seungil Huh, Sungeun Eom, Ryoma Bise, Zhaozheng Yin, and Takeo Kanade

Robotics Institute, Carnegie Mellon University 5000 Forbes Ave. Pittsburgh PA 15232, USA

ABSTRACT

Automated visual-tracking systems of stem cell populations in vitro allow for high-throughput analysis of time-lapse phase-contrast microscopy. In these systems, detection of mitosis, or cell division, is critical to tracking performance as mitosis causes branching of the trajectory of a mother cell into the two trajectories of its daughter cells. Recently, one mitosis detection algorithm showed its success in detecting the time and location that two daughter cells first clearly appear as a result of mitosis. This detection result can therefore helps trajectories to correctly bifurcate and the relations between mother and daughter cells to be revealed. In this paper, we demonstrate that the functionality of this recent mitosis detection algorithm significantly improves state-of-the-art cell tracking systems through extensive experiments on 48 C2C12 myoblastic stem cell populations under four different conditions.

Index Terms— Mitosis detection, Stem cell tracking, Cell image analysis, Cell lineage construction

1. INTRODUCTION

Automated systems for visual-tracking of cell populations *in vitro* have enormous potential for stem cell biology and stem cell engineering because these systems allow for high-throughput analysis of time-lapse microscopy images [1, 2, 3], whereas manual analysis is often intractable. In particular, cell tracking systems adopting phase-contrast microscopy are attractive due to its non-destructivity so that such systems enable continuous monitoring of live and intact cells. These tracking systems can provide quantitative analysis of stem cell behavior such as proliferation and migration, discovery of optimal conditions for stem cell expansion, as well as quality assurance/control measures of stem cell expansions.

Mitosis is the process whereby the genetic material of a eukaryotic cell is equally distributed between daughter cells through nuclear division. In automated cell tracking systems, mitosis detection is critical for tracking performance because cell division, which leads to the branching of tracking trajectories, is a major cause of tracking failure. Mitosis detection compensates for the failure of cell region segmentation due to

the changes in cell shape, size, and brightness during mitosis as well. With precise mitosis detection, quality cell lineage construction can also be achieved since the spatio-temporal information on cell birth helps to reveal the relation between mother and daughter cells.

Existing mitosis detection methods based on computer vision techniques that adopt phase-contrast microscopy timelapse microscopy images can be categorized into two groups: tracking-based methods [4, 5, 6, 7] and tracking-free methods [8, 9, 10, 11]. Tracking-based methods typically first track cells in the field of view; their morphological changes are then examined along the trajectories to detect mitosis [4, 5]. In other tracking-based methods, mother and daughter cell regions or their trajectories are first obtained; while they are linked to each other, mitotic events are implicitly or explicitly detected [6, 7]. Tracking-free methods often involve the learning of visual characteristics of mitotic cells based on human-annotated samples [8, 10, 11]. To reduce search space without tracking from large-sized original image sequences to small-sized patch sequences, several patch sequence construction schemes were also developed [9, 10, 11].

Recently, Huh *et al.* [11] proposed a mitosis detection approach for stem cell populations in phase-contrast microscopy images and demonstrated success in detecting *birth event*, which is defined as the time and location at which two daughter cells first clearly appear as a result of mitosis. After constructing candidate patch sequences based on brightness, a probabilistic model named Event Detection Conditional Random Field (EDCRF) was applied to determine whether and at which patch each candidate sequence contains a birth event. Experimental results on C3H10T1/2 and C2C12 stem cell populations showed that the effectiveness and efficiency of this approach.

In this paper, we present a cell tracking algorithm that incorporates the functionality of this mitosis detection algorithm. The birth event information provided by the mitosis detection can significantly improve the performance of cell tracking, resulting in more quality cell lineage construction. In experiments, we compare the systems involving and not involving the mitosis detection on 48 C2C12 myoblastic stem cell populations under four different conditions. These extensive experiments show that the precise birth event detection

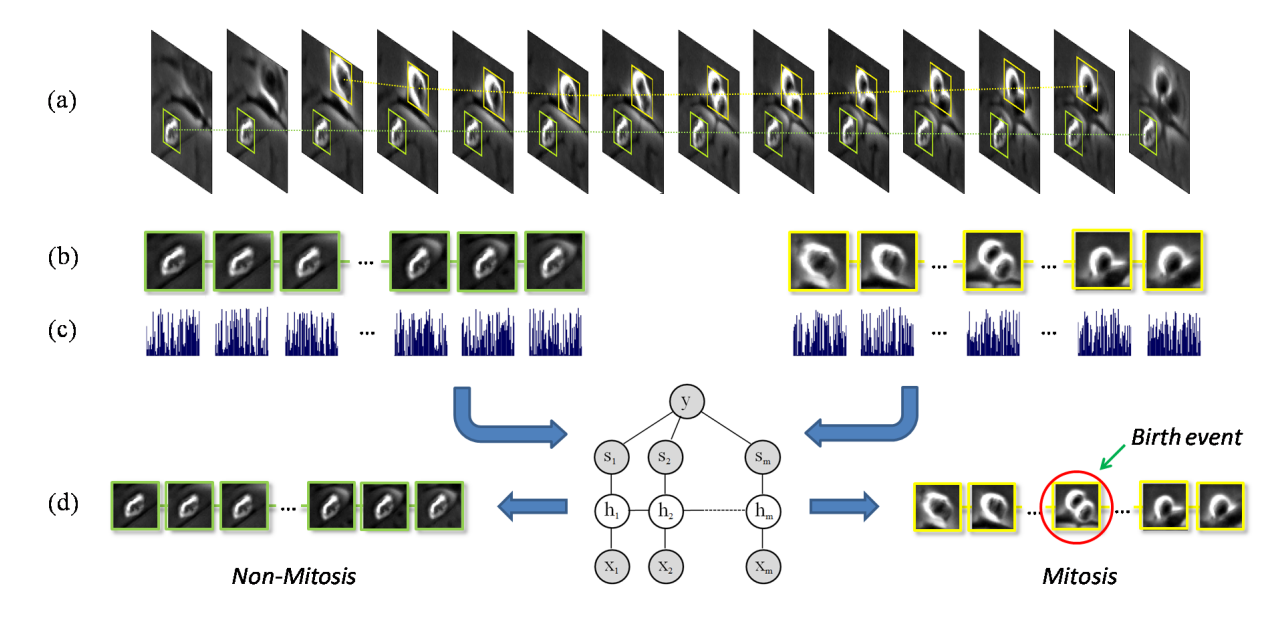


Fig. 1. Summary of the mitosis detection procedure [11]. (a) Candidate patch sequence extraction from consecutive phase-contrast microscopy image frames based on brightness. (The original images are much larger than these examples.) (b) Examples of candidate patch sequences. (c) Unique scale gradient histograms computed for each patch in candidate patch sequences. (d) Identification of mitosis occurrence and temporal localization of a birth event using Event Detection Conditional Random Field (EDCRF) [11].

considerably reduces false branching as well as more accurately identifies mother-daughter relations.

The remainder of this paper is organized as follows. We summarize the process of the mitosis detection algorithm [11] in Section 2. We then present a cell tracking system incorporating the functionality of this mitosis detection algorithm in Section 3. The experimental setup and results with discussions are presented in Sections 4 and 5, followed by conclusions in Section 6.

2. MITOSIS DETECTION

In this section, we briefly review the mitosis detection method [11], the functionality of which is adopted for our cell tracking system. For more details, we refer to [11].

Given a phase-contrast microscopy image sequence, the background of the images, which is simply computed as the average image of all images in the sequence, is subtracted from each image in order to correct intrinsic illumination variation in phase-contrast microscopy images. After background subtraction, candidate patch sequences, which may contain birth events, are extracted from the images as shown in Figures 1(a) and (b); as a result, mitotic events are spatially localized as well as the search space is significantly reduced. Specifically, bright square patches are first extracted from each image since mitotic cells are typically much brighter than non-mitotic cells. Candidate patch sequences are then constructed by linking spatially overlapped bright patches in

consecutive frames. The threshold of brightness for candidate patches is empirically set not to miss actual mitotic events.

After patch sequence construction, unique scale gradient histograms are computed as visual features for each candidate patch in the sequences as shown in Figure 1(c). Unique scale gradient histograms reflect the characteristics of phase-contrast microscopy images, resulting in good performance of mitosis detection. In detail, after dividing each patch into 4×4 subregions, gradient magnitudes weighted by a Gaussian function are accumulated into 4 bins along the orientations at each subregion. After $4\times4\times4=64$ features are computed for each patch, L2 normalization is applied to the feature vectors.

Now, the problem reduces to determining whether each candidate contains a birth event and which frame the birth event is located in. For these two decision tasks, a probabilistic model named Event Detection Conditional Random Field (EDCRF) was proposed. The graphical representation of EDCRF is illustrated in Figure 1(d).

Suppose that $\mathbf{x} = (x_1, x_2, \dots, x_m)$ is a candidate patch sequence that consists of m patches where x_j denotes the j-th patch (m can be varied for different sequences.). y is defined as the label of \mathbf{x} :

$$y = \begin{cases} p & \text{if the } p\text{-th patch of } \mathbf{x} \text{ contains a birth event} \\ 0 & \text{if there exists no birth event in } \mathbf{x} \end{cases}$$
 (1)

We assume hidden variables $\mathbf{h} = (h_1, h_2, \dots, h_m)$ and sub-labels $\mathbf{s} = (s_1, s_2, \dots, s_m)$ where h_j and s_j correspond to x_j . When a sequence label y is given, the sub-labels

 s_1, s_2, \cdots, s_m are defined as

$$s_{j} = \begin{cases} N & \text{if } y = 0 & \cdots \text{ no event} \\ B & \text{if } y > 0 \text{ and } j < y & \cdots \text{ before event} \\ A & \text{if } y > 0 \text{ and } j \ge y & \cdots \text{ after event} \end{cases}$$
 (2)

Under these definitions, we define a latent conditional model for sequence \mathbf{x} :

$$P(y|\mathbf{x}, \theta) = P(\mathbf{s}|\mathbf{x}, \theta) = \sum_{\mathbf{h}} P(\mathbf{s}|\mathbf{h}, \mathbf{x}, \theta) P(\mathbf{h}|\mathbf{x}, \theta)$$
(3)

where θ is a set of parameters of the model. This model can be further simplified by restricting that each sub-class label s is associated only with hidden states in a disjoint set \mathcal{H}_s as follows:

$$P(y|\mathbf{x},\theta) = \sum_{\mathbf{h}:\forall h_j \in \mathcal{H}_{s_i}} P(\mathbf{h}|\mathbf{x},\theta)$$
 (4)

where $P(\mathbf{h}|\mathbf{x},\theta)$ is defined using the typical conditional random field (CRF) formulation [12] with state and transition functions. We refer to [11] for the details.

Given n candidate patch sequence and label pairs $\{(\mathbf{x_1}, y_1), (\mathbf{x_2}, y_2), \cdots, (\mathbf{x_n}, y_n)\}$ as training samples, the following regularized log-likelihood function is maximized for learning parameters,

$$L(\theta) = \sum_{i=1}^{n} \log P(y_i|\mathbf{x_i}, \theta) - \frac{1}{2\sigma^2} ||\theta||^2$$
 (5)

where θ is a set of model parameters and σ is the variance of a Gaussian prior.

Given a new patch sequence \mathbf{x} consisting of m patches, conditional probabilities with all possible y, i.e., $P(y=0|\mathbf{x},\theta^*),\cdots$, and $P(y=m|\mathbf{x},\theta^*)$, can be computed as

$$P(y = 0|\mathbf{x}, \theta^*) = P(s_1 = N|\mathbf{x}, \theta^*) = \sum_{h_1 \in \mathcal{H}_N} P(h_1|\mathbf{x}, \theta^*),$$

$$P(y = 1|\mathbf{x}, \theta^*) = P(s_1 = A|\mathbf{x}, \theta^*) = \sum_{h_1 \in \mathcal{H}_A} P(h_1|\mathbf{x}, \theta^*),$$

$$P(y = j|\mathbf{x}, \theta^*) \quad \text{for } j = 2, ..., m,$$

$$= P(s_1 = B, \dots, s_{j-1} = B, s_j = A, \dots, s_m = A|\mathbf{x}, \theta^*)$$

$$= \sum_{h_{j-1} \in \mathcal{H}_B} P(h_{j-1}|\mathbf{x}, \theta^*) - \sum_{h_j \in \mathcal{H}_B} P(h_j|\mathbf{x}, \theta^*)$$
(6)

where θ^* is the optimal model parameter obtained from the training samples. Based on these probabilities, EDCRF simultaneously determines the occurrence of mitosis and the temporal location of the birth event as follows:

$$y^* = \begin{cases} 0 & \text{if } P(y = 0 | \mathbf{x}, \theta^*) > 0.5\\ \arg\max_{y=1,\dots,m} P(y | \mathbf{x}, \theta^*) & \text{otherwise} \end{cases}$$
(7)

3. CELL TRACKING SYSTEM

In this section, we present a tracking system that incorporates the functionality of the mitosis detection algorithm described in the previous section¹. For each phase-contrast microscopy image, blobs that are likely to correspond to cells are first segmented by a recently developed cell segmentation algorithm for phase-contrast microscopy [13].

Based on the segmented blobs, frame-by-frame data association is performed by considering hypotheses reflecting stem cell behaviors: migration, exit, entrance, clustering, and mitosis. More formally, let a_i be the i-th detected cell in the previous frame and b_j be the j-th blob in the current frame. Then, likelihoods of the five cases are computed as follows:

• one-to-one: a cell migrates in the field of view.

$$\ell_{1 \to 1}(a_i, b_j) = e^{-\frac{||f(a_i) - f(b_j)||}{\sigma}}$$
 (8)

• one-to-none: a cell exits from the field of view.

$$\ell_{1\to 0}(a_i) = e^{-\frac{d(a_i)}{\lambda}} \tag{9}$$

• none-to-one: a cell enters the field of view.

$$\ell_{0\to 1}(b_j) = e^{-\frac{d(b_j)}{\lambda}} \tag{10}$$

• many-to-one: multiple cells overlap.

$$\ell_{n\to 1}(a_{i_1}, \dots, a_{i_K}, b_j) = e^{-\frac{||f(\bigcup_{k=1}^K a_{i_k}) - f(b_j)||}{\sigma}} \quad (11)$$

• one-to-two: a cell divides into two cells

$$\ell_{1\to 2}(a_i, b_{j_1}, b_{j_2}) = e^{-\frac{||f(a_i) - f(b_{j_1} \cup b_{j_2})||}{\sigma}}$$
 (12)

where f(a) is a feature vector extracted from blob a, which consists of the center position of the blob, the Fourier descriptors of the blob contour, and the intensity histogram of the blob region; d(a) is the distance between the center of blob a and the image boundary; and σ and λ are free parameters. In order to reduce the number of hypotheses considered in frame-by-frame data association, we compute the likelihoods between the cells in the previous and current frames only when their distance is less than a certain threshold. Similarly, the hypotheses regarding cell exit and entrance are considered only for the cells which are located closely to the image boundary.

The birth event information detected by the mitosis detection algorithm [11] is used to establish hypotheses as follows.

¹It is worth mentioning that this system is an improved version of the cell tracking system developed by our group, which was recently introduced in [14], in that birth events are more accurately detected using EDCRF. In this paper, we describe our tracking system focusing on how mitosis detection contributes to cell tracking, which was not sufficiently analyzed nor discussed in [14].

The last hypothesis regarding mitosis often produces a high likelihood of cell division although no mitosis occurs, e.g., when a lost cell from cell detection/tracking appears closely to another cell or more than one blob region are detected within one cell during segmentation. On the other hand, the likelihood may sometimes be too low even though mitosis occurs, e.g., when cell region segmentation fails during mitosis due to the changes in cell shape, size, and brightness and detects daughter cell regions after the cells move away from the birth event location. To resolve these confusions, we first explicitly detect birth events using the mitosis detection algorithm. For each birth event, we then find the nearest cell from the birth location and change its status as potentially mitotic in several following frames. The mitosis hypothesis is considered only for these potentially mitotic cells. The several frame delay is allowed because daughter cells are often attached to each other in several frames right after the birth event; automated detection and segmentation methods can hardly separate individual cells in such a case.

After obtaining all hypotheses between two consecutive frames, we find the best combination of hypotheses as follows. Suppose that there are N_1 cells and N_2 blobs in the previous and current frames, respectively, and M hypotheses are established between the two frames. We build a matrix $C = [C_{ij}]$, which is an $M \times (N_1 + N_2)$ binary matrix where $C_{ij} = 1$ if and only if the i-th hypothesis is involved with the j-th element of the union of N_1 cells and N_2 blobs. We then solve the following integer programming problem.

$$\arg\max_{x} \ p^{T}x$$

$$s.t. \ (C^{T}x)_{i} \leq 1 \quad for \ i = 1, \cdots, N_{1} + N_{2}$$

$$x_{i} \in \{0, 1\} \quad for \ j = 1, \cdots, M$$

$$(13)$$

where p is an $M \times 1$ vector containing all the likelihoods and $(C^Tx)_i$ is the i-th element of C^Tx . Solving this optimization problem yields an $M \times 1$ binary vector x where $x_i = 1$ indicates that the i-th hypothesis is selected as an element of the best combination. Note that each cell or blob can be selected at most once due to the constraint $(C^Tx)_i < 1$.

After the best association is found, if there are remaining cells in the previous frame, the cells are considered again for the association between the next two frames. In other words, the cells are assumed to be undetected in the current frame and expected to be detected in the following frame. If a track is continuously not linked with a cell for 10 frames, the track is eliminated. As to each of the remaining cells in the current frame, we investigate its neighboring cells. If there is a potentially mitotic cell nearby, the remaining cell is linked with the potentially mitotic cell as a daughter cell; otherwise, a temporary track initiates from the remaining cell. Each temporary track is confirmed as a real track after 10 frames if the track is linked with cells in most of the 10 frames.

4. EXPERIMENTS

4.1. Data and Ground truth

During the growth of stem cells, phase-contrast microscopy cell images were acquired every 5min using a Zeiss Axiovert T135V microscope (Carl Zeiss Microimaging, Thornwood, NY) equipped with a 5X, 0.15 N.A. phase-contrast objective, a custom-stage incubator, and the InVitro software (Media Cybernetics Inc., Bethesda, MD).

In order to obtain training samples of birth events, one phase-contrast microscopy image sequence of C2C12 cells consisting of 1013 images (approx. 84.4hrs) was acquired under control condition. For evaluation of tracking performance, twelve image sequences of C2C12 cells were acquired under each of four different conditions: control, FGF2, BMP2, and FGF2+BMP2; as a result, total 48 image sequences, each of which consists of 600 images (50hrs), were acquired. Each of these images contains 1392×1040 pixels with a resolution of 1.3μ m/pixel.

Manual annotation of birth events was performed on the first long C2C12 image sequence; as a result, total 673 birth event samples were obtained. For each birth event, the center of the boundary between the two daughter cells was marked when the boundary is first clearly observed. In order to evaluate tracking performance, for each of 48 sequences, three cells are randomly selected in the initial frame and the cells and their progeny cells are manually tracked. For manual tracking, the center of each cell is marked.

4.2. Evaluation

To measure the contribution of the mitosis detection to cell tracking, we compare the performances of two tracking systems: tracking systems without and with the mitosis detection. For the tracking system without mitosis detection, the hypothesis regarding mitosis is considered for every cell and a temporary track initiates from every remaining cell in the current frame after association due to the absence of information on mitosis occurrence and location.

To evaluate the performance of tracking systems, we measure how much effort is required to obtain the perfect cell lineage tree from the lineage tree constructed by tracking algorithms; lineage tree construction is one of the most important goals of cell tracking. To quantitatively calculate this effort, we consider four types of errors: missed mother-daughter relations, switched tracks, untracked frames, and mistracked frames. Figure 2 illustrates these four types of errors. To obtain the perfect cell lineage from tracking results, all of these errors are required to be fixed.

Among these errors, we count the occurrences of the first two errors, missed mother-daughter relations and switched tracks, since they are related to mitosis detection. If actual mitosis is not detected, the trajectory of the mother cell does not branch and thus the relation between mother-daughter cells

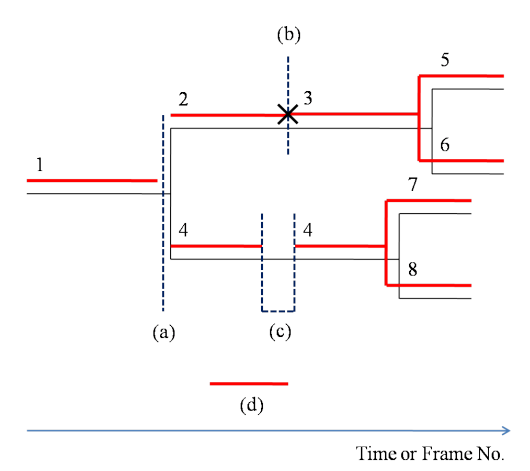


Fig. 2. Illustration of four types of errors that need to be fixed to obtain the perfect lineage tree from tracking results: (a) missed mother-daughter relations (1-2 and 1-4), (b) switched track (from 2 to 3), (c) untracked frames (between two 4s), and (d) mistracked frames. The lineage tree consisting of black thin lines represents ground truth. The red thick lines above the ground truth lineage tree represent tracking results. The numbers above tracks indicate track IDs. Among these

errors, the errors (a) and (b) are related to mitosis detection.

is not captured. On the other hand, if mitosis is incorrectly detected when no mitosis occurs, the trajectory of the cell wrongly branches and thus the track of the cell is switched. When considering mother-daughter relations, we allow ten frame delay because the regions of two daughter cells are hard to be separately identified right after cell division. In other words, mother-daughter relations are considered to be missed if they are not discovered within ten frames after the daughter cells are born. The other two errors, untracked frames and mistracked frames, are not relevant to mitosis detection, but to cell region detection and segmentation; thus, these errors remain regardless of mitosis detection. Since the objective of this paper is to show the contribution of mitosis detection to cell tracking systems, we do not report these errors.

5. RESULTS AND DISCUSSIONS

Cell tracking accuracy significantly increased after incorporating the birth event information provided by the mitosis detection algorithm [11]; the numbers of missed mother-daughter relations and switched tracks were considerably reduced as shown in Figure 3 and Table 1. Compared to the tracking system without mitosis detection, the system with mitosis detection achieved on average 39%, 28%, 51%, and 46% improvements in detecting mother-daughter cell relations and 16%, 11%, 30%, and 26% improvements in reducing switched tracks for control, FGF2, BMB2, and FGF2+BMP2 conditions, respectively. In total, 42% and

21% improvements were achieved in terms of these two measures. The *p*-values obtained by ratio paired *t*-tests confirm that these improvements are statistically significant. The performance improvement in terms of missed mother-daughter relations is greater than that of switched tracks because tracking switching is only partially related to mitosis detection in that it can occur in other situations, such as cell overlapping.

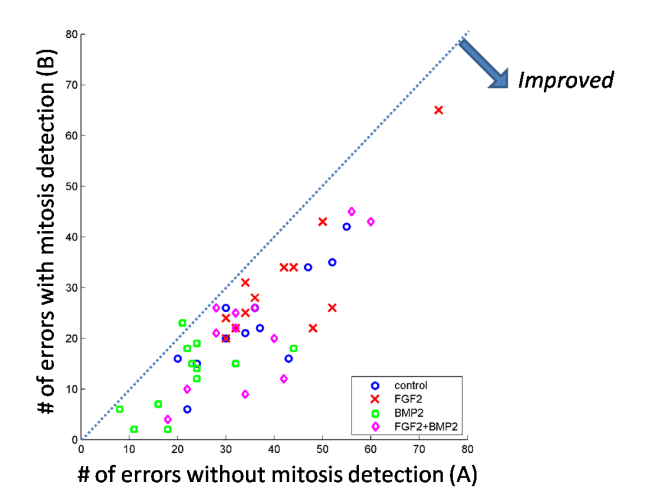
The advantages of precise mitosis detection in cell tracking systems can be summarized as follows. First, precise mitosis detection reduces the numbers of undetected mitosis as well as mitosis candidates. Without mitosis detection, much more hypotheses regarding mitosis may be established, which degrades the efficiency of cell tracking systems, particularly when cells are clustered together. In addition, mitosis which is not captured by the association with the mitosis hypothesis can be detected in the track maintenance step if mitosis detection is involved. Second, mitosis detection is helpful to correctly identify a mitotic cell and the mother-daughter relations. Without mitosis detection, a neighboring cell is often determined as a mother cell particularly when the cell is in contact with one of the daughter cells; on the other hand, precise information on birth location identifies a real mitotic cell. Lastly, mitosis detection makes cell tracking more robust to incorrect segmentation. In segmentation, artifacts or parts of background are often detected as cell regions; in addition, one cell is sometimes detected by more than one cell region. If either case lasts for several frames, a mitosis hypothesis is generally considered with a high likelihood to handle additional cell regions. Mitosis detection avoids track switching by excluding the mitosis hypothesis in such situations.

The lineage tree in Figure 4(a) clearly demonstrates that undetected and incorrectly detected mitosis are major causes of tracking failure. The precise birth event detection reduces missed mother-daughter relations due to undetected mitosis as well as false branching due to incorrectly detected mitosis, resulting in more accurate tracking and lineage construction as shown in Figure 4(b). Figure 5 shows sample images illustrating the tracking results of the systems without and with mitosis detection. As shown in the figure, the tracking system with mitosis detection correctly reveals mother-daughter relations when another cell is located nearby and cell segmentation is incorrectly performed while the tracking system without mitosis detection fails.

6. CONCLUSIONS

In this paper, we show that cell tracking systems can be considerably improved by the mitosis detection that precisely localizes the time and location of cell birth. Extensive experiments on 48 C2C12 stem cell populations clearly demonstrate that mitosis detection helps to avoid false branching of cell tracking as well as more accurately reveal mother-daughter relations, significantly improving tracking performance and reducing human effort to construct quality stem cell lineages.

Error (a): Missed mother-daughter relation



Error (b): Switched track

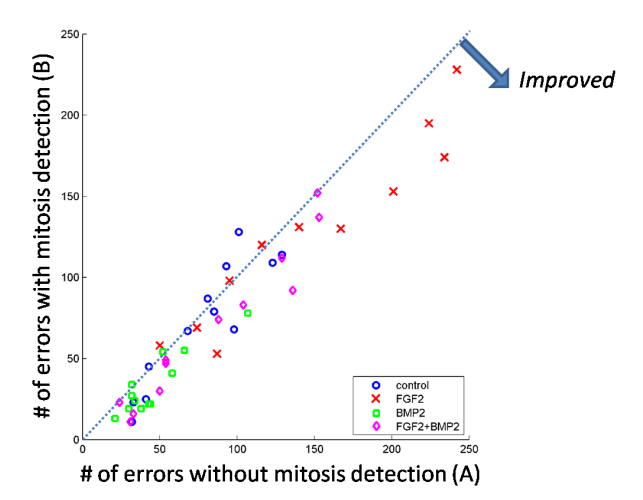


Fig. 3. Tracking performance comparison between tracking systems without (x-axis) and with (y-axis) mitosis detection in terms of the numbers of missed mother-daughter relations (left) and switched tracks (right). The points below the diagonal lines indicate that tracking is improved through the mitosis detection. After the mitosis detection is incorporated, missed mother-daughter cell relations and switched tracks were reduced in 47 out of 48 sequences and in 37 out of 48 sequences, respectively.

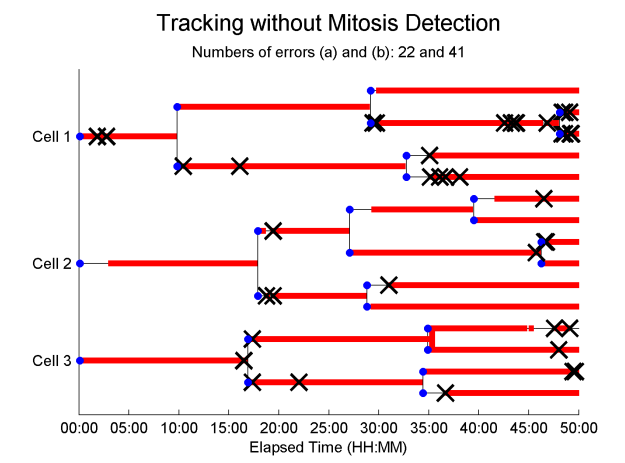
Error (a): missed mother-daughter relation					
	Control	FGF2	BMP2	FGF2+BMP2	Total
Geometric mean of error ratios (B/A)	0.61	0.72	0.49	0.54	0.58
Geometric STD of error ratios (B/A)	1.37	1.23	1.87	1.60	1.58
p-value	0.0002	0.0001	0.0014	0.0006	< 0.0000
Error (b): switched track					
	Control	FGF2	BMP2	FGF2+BMP2	Total
Geometric mean of error ratios (B/A)	0.84	0.89	0.70	0.74	0.79
Geometric STD of error ratios (B/A)	1.41	1.19	1.28	1.35	1.33
<i>p</i> -value	0.0560	0.0209	0.0003	0.0035	< 0.0000

A: number of errors without mitosis detection, B: number of errors with mitosis detection

Table 1. Tracking performance comparison between tracking systems without and with mitosis detection in terms of the geometric mean and STD of the error ratios. When the mitosis detection is incorporated, the number of missed mother-daughter relations was reduced on average by 39%, 28%, 51%, and 46%; the number of switched tracks by 16%, 11%, 30%, and 26% in control, FGF2, BMP2, and FGF2+BMP2 conditions, respectively; in total, 42% and 21% performance improvements were achieved in terms of the numbers of errors (a) and (b), respectively. The *p*-values obtained by ratio paired *t*-tests show that these performance improvements due to the mitosis detection is statistically significant.

7. REFERENCES

- A.J. Hand, T. Sun, D.C. Barber, D.R. Hose, and S. Macneil, "Automated tracking of migrating cells in phase-contrast video microscopy sequences using image registration," *J. Microsc.*, 234(1):62-79, 2008.
- [2] K. Li, E.D. Miller, M. Chen, T. Kanade, L.E. Weiss, P.G. Campbell, "Cell Population Tracking and Lineage Construction with Spatiotemporal Context," *Med. Image Anal.*, 12(5):546-66, 2008.
- [3] D. House, M.L. Walker, Z. Wu, J.Y. Wong, and M. Betke, "Tracking of Cell Populations to Understand their Spatio-Temporal Behavior in Response to Physical Stimuli," in Proc. IEEE Conference on Computer Vision and Pattern Recognition Workshop on Mathematical Methods in Biomedical Image Analysis, pp. 186-93, 2009.
- [4] F. Yang, M.A. Mackey, F. Ianzini, G. Gallardo, and M. Sonka, "Cell Segmentation, Tracking, and Mitosis Detection using Temporal Context," in Proc. International Conference on Medical Image Computing and Computer Assisted Intervention, pp. 302-9, 2005.
- [5] O. Debeir, P. Van Ham, R. Kiss, and C. Decaestecker, "Tracking of Migrating Cells under Phase-Contrast Video Microscopy with Combined Mean-Shift Processes," *IEEE Trans. Med. Imag.*, 24(6):697-711, 2005.
- [6] O. Al-Kofahi, R.J. Radke, S.K. Goderie, Q. Shen, S. Temple, and B. Roysam, "Automated Cell Lineage Construction: A Rapid Method to Analyze Clonal Development Established with Murine Neural Progenitor Cells," Cell Cycle, 5(3):327-35, 2006.
- [7] D. Padfield, J. Rittscher, N. Thomas, and B. Roysam, "Spatio-temporal



Cell 2 O0:00 05:00 10:00 15:00 20:00 25:00 30:00 35:00 40:00 45:00 50:00 Elapsed Time (HH:MM)

Fig. 4. Lineage tree comparison between the tracking systems without (left) and with (right) the mitosis detection on the first C2C12 sequence under control condition. The thin black lineage trees are constructed by manual annotation. The red thick lines covering the ground truth lineage trees represent tracking results. Two types of errors were counted: (a) missed mother-daughter relation, a pair of which are shown as a vertical black line not covered with a red line, and (b) switched track, which is indicated by an X mark. These examples clearly show that the mitosis detection significantly reduces these two types of errors in cell tracking and lineage construction.

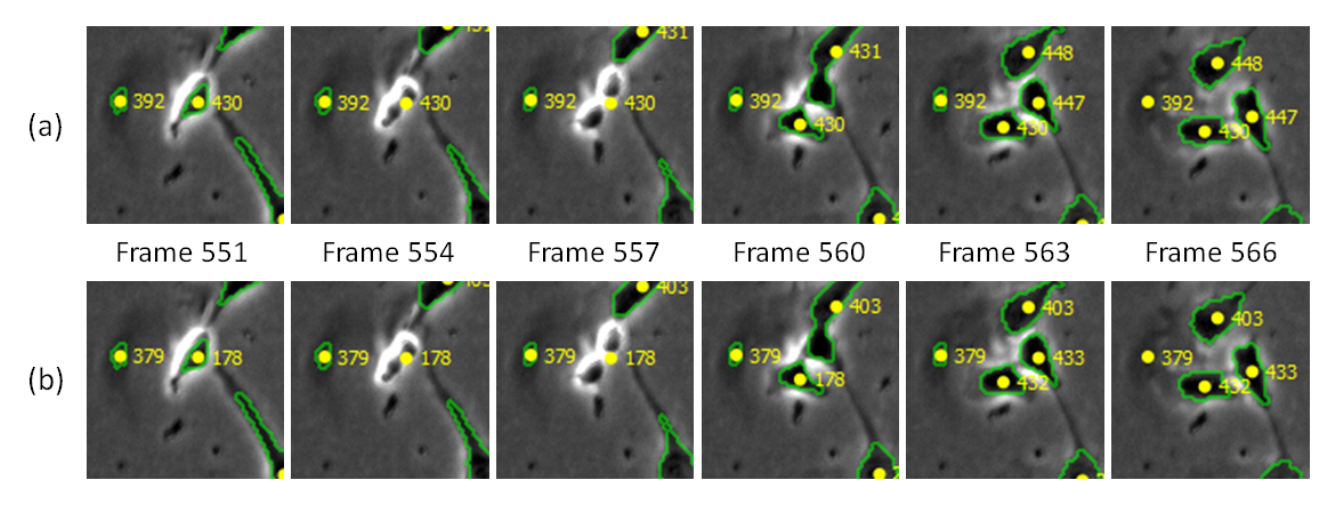


Fig. 5. Example images illustrating cell tracking results of the tracking systems (a) without and (b) with mitosis detection. A birth event occurs at frame 557. After the birth event, the system without the mitosis detection incorrectly detects mother-daughter relations; between frames 560 and 563, cell 431 is detected as a mother cell and cells 447 and 448 as its daughter cells due to the incorrect segmentation at frame 560. Despite such a situation, the system with the mitosis detection correctly reveals the mother-daughter relation (cell 178 as a mother cell and cells 432 and 433 as its daughter cells) since the time and location of the birth event detected by the mitosis detection method are incorporated into the system.

- cell cycle phase analysis using level sets and fast marching methods," *Med. Image Anal.*, **13**(1):143-55, 2009.
- [8] K. Li, E.D. Miller, M. Chen, T. Kanade, L.E. Weiss, and P.G. Campbell, "Computer Vision Tracking of Stemness," in *Proc. IEEE International Symposium on Biomedical Imaging*, pp. 847-50, 2008.
- [9] O. Debeir, V. Mégalizzi, N. Warzée, R. Kiss, and C. Decaestecker, "Videomicroscopic extraction of specific information on cell proliferation and migration in virto," Exp. Cell Res., 314(16):2985-98, 2008.
- [10] A-A Liu, K. Li, and T. Kanade, "Mitosis Sequence Detection using Hidden Conditional Random Fields," in *Proc. IEEE International Sym*posium on Biomedical Imaging, 2010.
- [11] S. Huh, Dai Fei E. Ker, R. Bise, M. Chen, and T. Kanade, "Automated Mitosis Detection of Stem Cell Populations in Phase-Contrast Microscopy Images," *IEEE Trans. Med. Imag.*, 2011.
- [12] J. Lafferty, A. McCallum, and F. Pereira, "Conditional random fields: probabilistic models for segmenting and labelling sequence data," in *Proc. International Conference on Machine Learning*, pp. 282-9, 2001.
- [13] Z. Yin, K. Li, T. Kanade, and M. Chen, "Understanding the Optics to Aid Microscopy Image Segmentation," *Medical Image Computing and Computer Assisted Intervention*, 2010.
- [14] T. Kanade, Z. Yin, R. Bise, S. Huh, S. Eom, M. Sandbothe, and M. Chen, "Cell Image Analysis: Algorithms, System and Applications," in Proc. IEEE Workshop on Applications of Computer Vision, 2011.